Precision coating of ocular devices/contact lenses by nanoelectrospray additive printing

Chak Hin Tam [a], Matthew S. Alexander [b], Sheng Qi [a],*

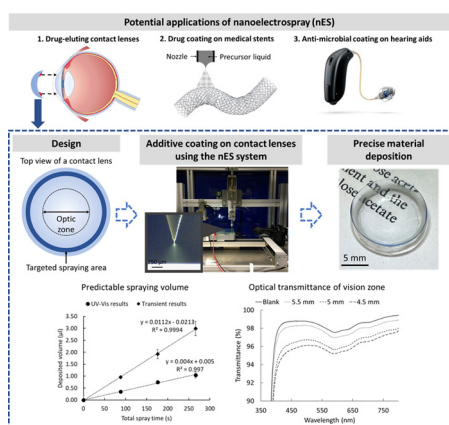[a] School of Pharmacy, University of East Anglia, Norwich, UK
[b] School of Engineering, University of East Anglia, Norwich, UK

HIGHLIGHTS

- For the first time, a novel nanoelectrospray additive coating system is demonstrated that is capable patterning polymer-drug films at the periphery of commercial contact lenses and avoid coverage of the visual axis.
- The nanoelectrospray system deposits micro- to nano-litre of polymer solution precisely in pre-defined patterns with typical width of 2 mm at the peripheral region on the soft, wet and curved hydrogel contact lens.
- The patterned nanoelectrospray coating leaves excellent optical transparency (>95%) in the optical zone of coated contact lenses.
- The spray volume can be monitored and estimated by using established scaling laws and the spray current transient to ensure the accurate material dosing.

GRAPHICAL ABSTRACT

ARTICLE INFO

ABSTRACT

Eye drops are widely used for treating ocular diseases, but with poor bioavailability less than 5%. Drug-eluting contact lenses (DECLs) have been proven to improve the efficacy of treatment. For the manufacturing of DECLs, no method can directly deposit drug formulation on commercial lenses. In this work, a novel additive manufacturing approach, nanoelectrospray (nES), and a custom-built nES printing system was developed to directly deposit drug formulations on the surfaces of commercial contact lenses. As a demonstration, nES was used to coat the model biopolymer, zein, onto commercial lenses. Precise deposition of a ring-shaped polymer layer only on the peripheral region was achieved. For printing optimisation, the spraying width is primarily controlled by the nozzle substrate distance. The coating thickness, which can be used to directly control the drug dose, is subject to the polymer concentration in the formulation, dosing speed and the number of rotations. By using the spray current transient and established scaling law, the predicted spray volume is highly correlated to the experimental results. This study built a

---

* Corresponding author.
   E-mail addresses: chak-hin.tam@uea.ac.uk (C.H. Tam), matthew.alexander@uea.ac.uk (M.S. Alexander), sheng.qi@uea.ac.uk (S. Qi).

firm technological foundation for using nES as a novel additive manufacturing method to produce DECLs with drug coating at the surfaces of contact lenses in pre-defined patterns and locations.

1. Introduction

Ocular medications are commonly given in the form of eye drops. Eye drops are self-administered directly to the eye, but many patients struggle to use eye drops properly. More importantly, the bioavailability of eye drops is often limited to 5% [1] due to the drug loss via tear clearance and drainage from the eye [2]. This leads to frequent instillation of eye drops to maintain the drug concentration at the therapeutic level in the eye [3]. Additionally, eye drops have been reported to have poor patient adherence [4,5], preservatives induced eye irritation and intolerance [6], highly variable dosing [7,8] and poor drug absorption [2].

Drug-eluting contact lenses (DECLs) were explored as an alternative drug delivery method to overcome the limitations of eye drops. DECLs are estimated to improve the bioavailability to 50%, in comparison to 5% by eye drops [9]. The concept of DECLs was first established in the 1960s and Johnson & Johnson Vision launched the first commercial DECLs in 2021 [10,11]. These DECLs contain ketotifen fumarate for treating ocular itchiness associated with allergies during contact lens wear. These contact lenses are soaked into the drug-loaded saline solution with a pre-defined drug concentration [12,13]. Loading ketotifen to the contact lens relies on electrostatic adsorption of drug molecules into the lens material and is highly drug specific, and not applicable to many other ocular drugs. In addition, the method is highly wasteful and the release of drugs from the soaked lenses is often rapid and uncontrolled. Other drug loading methods include molecular imprinting [14], sandwiching drug-loaded polymer films in the polymer matrix of the contact lens [15], and immersion of contact lenses into supercritical fluid [16]. These methods require either development of new polymer chemistry or the implementation of a new and complex multi-step manufacturing process. The intrinsic physical properties of contact lenses are often affected by the above methods [17]. Far-field electrospinning was reported to coat drug layers non-selectively on the lens surface, and therefore, required masking of the vision zone [18]. Currently, there is no reported effective additive manufacturing method that can be readily adopted by the existing contact lens manufacturing process and is suitable for high volume production of DECLs.

In this paper, the design, working principle, characterisation and optimisation of nanoelectrospray (nES), a new platform coating technology that can be used to coat CLs with polymer/drug formulations to product DECLs, are detailed. A widely range of synthetic and natural polymers can be processed by nES, with examples including poly(lactic-co-glycolic acid), ethylene-vinyl acetate, polycaprolactone, polylactic acid, zein, chitosan and hyaluronic acid. The processability of a polymer solution for nES is highly dependent on the electrical conductivity and viscosity of the precursor solution [19]. The conductivity depends on the solvent system and intrinsic property of the polymer [20]. The viscosity of a polymer solution is subject to the polymer concentration and molecular weight of the polymer, which also has influence on the morphology of coating [21]. The molecular weight cut-off of a polymer is considered individually to generate coatings with desired morphology [22].

The nES utilises a miniature spraying method that allows layer-by-layer drug deposition with flexible dosing and placement precision for rapid production of DECLs using commercially available CLs. The nES system enables the on-demand deposition of a thin layer of polymeric coating onto the peripheral area of the contact lens to preserve the vision zone, aiming to mitigate its influence on the intrinsic physical properties of the contact lens. These features mean that nES is a less wasteful method since all the sprayed materials are transferred onto the contact lens and have the potential to deposit tailored doses of medications. Various drugs can be coated by nES on different types of commercially available CLs to prepare DECLs for treating ocular diseases. Additionally, the technology would be readily integrated into the current manufacturing lines for CLs.

1.1. Principle of nES

The nES process involves the application of an electric field to the working fluid, commonly held in a capillary tube, to overcome the surface tension and initiate the ejection of a charged liquid jet which can subsequently break up into a plume of charged droplets (Fig. 1). The nES process shares the same working principle as electrospray and electrospinning, but in nES, the sprayed liquid flow rate is dictated solely by the applied electric field and in the absence of applied voltage, no flow or liquid ejection from the nozzle occurs [23,24]. Similar to conventional electrospray, nES can operate in several modes including the most studied stable cone-jet mode (which occurs over a limited range of field strength and flow rate) and may also exhibit quasi-steady pulsating spray modes [25]. Key to nES printing, the precise control of nES in a drop-on-demand fashion has also been demonstrated [26], where minute volumes, as low as femtolitres, were reproducibly isolated and deposited onto a substrate. These benefits have led to the application of nES printing in many fields including the fabrication of conductive interconnects [27], touch-screen sensors [28], tissue engineering scaffolds [29,30],light-emitting devices [31] and possi-
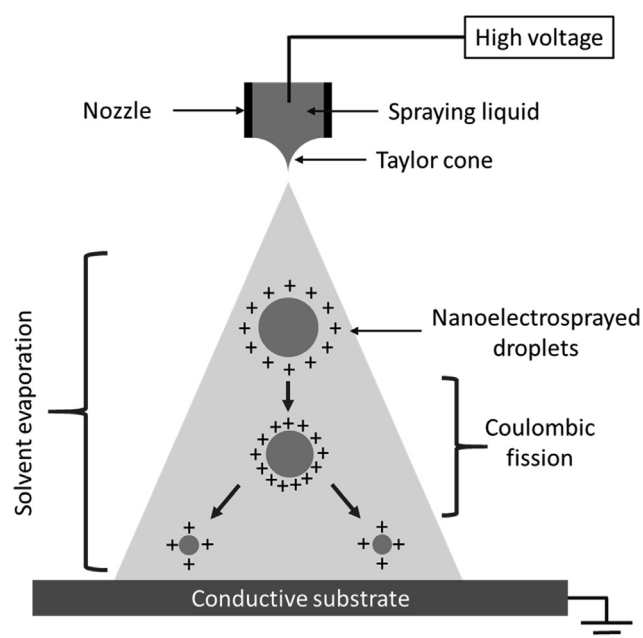

Fig. 1. Illustration of the nES process. The flow rate depends on the applied voltage and no syringe pump is required in the experimental setup.

bly surface modification for soft hydrogel[32]. In nES, previous work has shown that the lowest liquid throughput rates are achieved at low field strength (at field strength below the threshold for stable cone-jet mode and where pulsation modes are observed) where pulsation modes are observed.

The volume ejected during a single pulsation event is related to the total charge ejected as described by Paine et al. [26];

$$v_{est} = \frac{\tau_{on}\epsilon}{\gamma K}\left(\frac{I_{DC}}{f(\epsilon)}\right)^2 \tag{1}$$

where τ_{on} is the on-time, γ is surface tension, K is the conductivity of the solution, I_{DC} is calculated by integrating under the current transient to estimate the charge per cycle, then dividing by the number of pulsation events, and $f(\epsilon)$ is a function given by De La Mora and Loscertales [33,34]. By switching the applied voltage rapidly between a lower level where no liquid ejection occurs to a higher value above the voltage required for nES onset, the number of pulsation events occurring could be controlled by the dwell time at the higher potential.

In this study, zein was used as the model coating polymer due to its good film-forming properties with a wide range of biomedical applications [35,36]. It is biocompatible, biodegradable and classified by the U.S. Food and Drug Administration as a generally recognised safe (GRAS) polymer [37].

This study aims to demonstrate the capability of the bespoke nES printing system using zein as the polymer candidate. The influence of nES spraying parameters and liquid physical properties, such as nozzle-to-substrate distance, print nozzle travelling velocity (dosing speed), liquid conductivity and viscosity on the width, thickness and polymer coating profile on glass and contact lens substrates. The effect of zein concentration on the quality of patterned coating was also investigated. Estimation of the spray volume of zein solution was performed using two independent methods; one based on established scaling laws and measured current transients during spray coating and the other from the dissolution of printed films and spectroscopic measurements, to enable comparison of theoretically based estimates with experiment. To the best of our knowledge, this is the first report on using nES, as an additive manufacturing method, for on-demand patterned liquid deposition with high precision on commercial soft contact lenses. This study set the technological foundation for the potential biomedical applications of nES for coating and drug deposition on the surfaces of medical devices.

2. Materials and methods

2.1. Materials

Purified zein was obtained from Thermo Scientific (Loughborough, UK). Ethanol absolute was sourced from VWR Chemicals (Lutterworth, UK). Milli-Q (Millipore, Merck, USA) ultra-pure water was used to prepare all aqueous solutions. Phosphate buffer saline (PBS) tablets pH 7.4 and fluorine-doped tin oxide glass slides were purchased from Sigma-Aldrich (Gillingham, UK). Commercial soft contact lenses, Biomedics 55 contact lenses, with a composition of 45% ocufilcon D/55% water, were used (CooperVision Ltd, Fareham, UK). All materials were obtained from suppliers without further processing.

2.2. Preparation and physical characterisation of zein solutions for nES

The 2.5% w/v and 5% w/v zein solutions were prepared by dissolving the required amount of zein powder in either 70% or 80% w/w aqueous ethanol using a vortex mixer at ambient conditions until all powder dissolved. The solution was filtered by a 0.45 μm PES syringe filter (Fisher Scientific, Loughborough, UK)

before nES. The conductivity, viscosity, surface tension, and density of the zein solution were measured following the methods below.

Conductivity measurements were performed at 25 °C by using the Jenway 4510 conductivity meter (Stone, UK) equipped with a microvolume conductivity probe (027816, Jenway, Stone, UK). Dynamic viscosity of the solutions was measured by a Discovery HR-2 rheometer (TA Instruments, Delaware, USA) equipped with a 2°, 40 mm cone-and-plate geometry. The method was set to be a flow ramp procedure from 0.1 to 100 s^{-1} at 25 °C for 60 s. The measurement was done in triplicate to calculate the average viscosity at 80 s^{-1} for comparison since zein in the aqueous ethanol showed non-Newtonian behaviour. The surface tension of the solutions was measured by a DMS-401 tensiometer (Kyowa, Niiza-City, Japan) using the pendant drop method. Ten measurements were carried out for each sample to calculate the average surface tension. The density of the solutions was measured by a DMA 4500M density meter (Anton Paar GmbH, Graz, Austria) equipped with an oscillating U-tube at 25 °C. The measurement was done in triplicate to calculate the average density.

2.3. Experimental setup of the nES printing system

The custom-made nES printer (PCE Automation, Beccles, UK) shown in Fig. 2. was built to automate the nES process to fabricate circular films or dots on surfaces. Within the system, a ceramic nozzle with a 50 μm internal diameter (MicroDot tip 7364054, Nordson EFD, Dunstable, UK) was connected to a 2.5 ml Luer lock syringe (Terumo, Japan), which is fixed to the motorised z-translation stage (EGSC-BS-KF-32-100-8P, Festo, Esslingen am Neckar, Germany) and travels vertically. Pneumatic pressure supplied to the syringe can be regulated by the in-line pressure gauge, which enables nES printing of highly viscous liquid. A digital camera with a high magnification lens (MVL6X12Z, Thorlabs LTD, Lancaster, UK) was used to monitor the spraying process. The fluorine-doped tin oxide glass slide was secured and grounded on the 2-dimension motorised x-y translation stage (5155-1000A, Festo, Esslingen am Neckar, Germany), which moves simultaneously to generate circular movements. The substrate is interchangeable with other substrate materials such as metal or insulators if required. All the movement in x, y and z directions and spraying parameters are controllable from the built-in control panel of the machine. There are a few components connected to the nES system externally. The high voltage power supplies (HCP 14-6500, F.u.G. Elektronik GmbH, Schechen, Germany) were connected to the high voltage switch (PVX-4140, Direct Energy, Inc., Colorado, USA), which is linked to the nES printer and responsible for switching voltage to get into pulsation mode. The function generator (TG 1000, Aim-TTi, Huntingdon, UK) was used to control the frequency and amplitude of the square waves generated. A current amplifier, (DLPCA – 200, Laser Components, Chelmsford, UK) was used to amplify the voltage and connected to a digital storage oscilloscope (TBS1104, Tektronix, Beaverton, USA) to monitor the waveform of the spraying process. The measurement resistance of the amplifier was set to 10^6 Ω for all measurements.

The initiation of nES can be controlled by switching the applied voltages. The V_1 voltage is the lower voltage which is below the onset voltage of nES. The spray only initiates at a voltage higher than the onset voltage (V_2) as shown in Fig. 3. By adjusting the difference between V_1 and V_2, the time required for charging the spraying liquid can be shortened. The V_1 was set to zero in all experiments to reduce variables. Direct current was adopted in all experiments.

2.4. Calculation of nES deposition volume

The procedure for analysis of the nES current transients to estimate the volume of solution deposited during the printing cycle
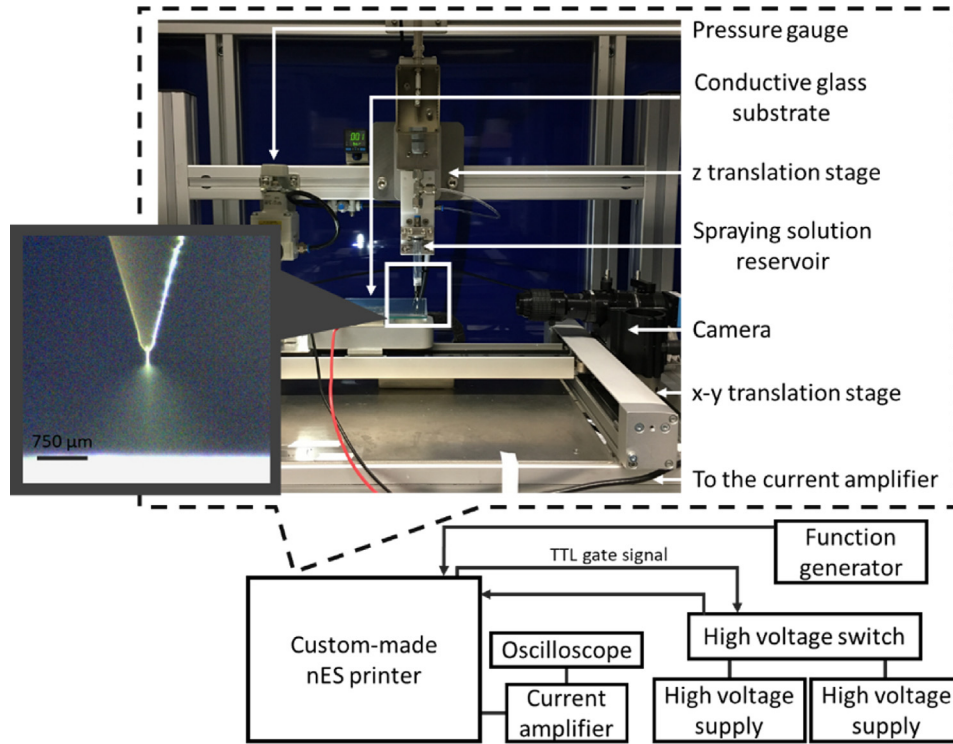
Fig. 2. Experimental setup of the custom-made nES system to deposit atomised polymer droplets on the substrates.
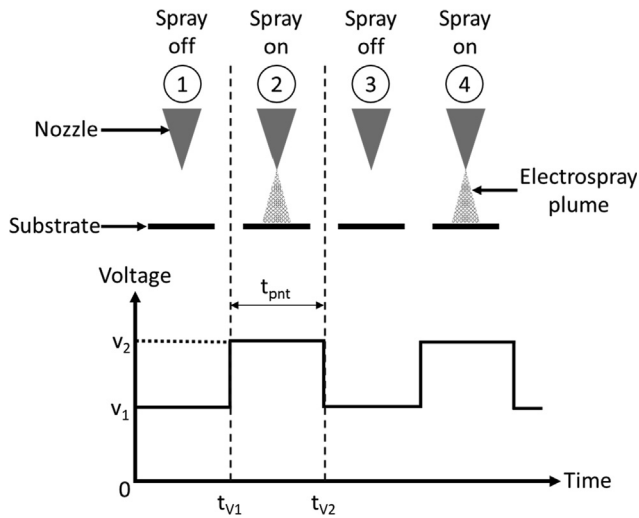

Fig. 3. Illustration of the switching of voltages to control the spray of nES.

was adapted from earlier work [26] and is briefly described here. An inline flowmeter was not used and instead the flow rate during nES printing was estimated by combining spray current transients, recorded by a fast current amplifier, with the established electrospray scaling laws. According to Fernandez de la Mora [33], the nES transient jet can be considered steady if the jet lifetime, τ_{on}, is longer than the electrical relaxation time, τ, where $\tau = \frac{\varepsilon \varepsilon_o}{K}$ and ε_o is the permittivity of free space. For the solutions used in this work, values for τ range from 1.04×10^{-8} s to 1.61×10^{-8} s, far shorter than any jet lifetime observed, which were typically 50–100 μS as indicated from the current transients. The second condition is that the jet diameter is less than the nozzle diameter. The jet diameter in the present work was always observed to be significantly smaller than the nozzle diameter, as illustrated by the

example inset image in Fig. 2 where the jet diameter is approximate 1/10th the size of the nozzle. Having satisfied these conditions, the rearranged scaling law expression previously described in equation (1) [26] can be used to estimate the volume ejected during a single pulsation, v_{est}.

In this process, the spray current transient, an example of which is shown in Fig. 4 below, can be approximated to a square wave with a duration τ_{on} where $\tau_{on} = (t_2 - t_1)$ and amplitude I_{DC}, where

$$I_{DC} = \frac{\int_{t_1}^{t_2} I.dt}{(t_2 - t_1)} .$$

The value of I_{base} was determined by averaging the current values from just before the steep rise in current at the onset of the transient pulse and was taken from an average of around 20 datasets. Then I_{peak} was measured as the highest current level reached in the transient and was also taken as the average of 20 measurements. The time threshold for t_1 and t_2 were taken at the points on the rising and falling current transient where the current level satisfied the condition $I > [0.25(I_{peak} - I_{base}) + I_{base}]$.

Three consecutive peaks were taken to calculate the average time required to perform one complete ejection period, τ_p, where $\tau_p = (\tau_{on} + \tau_{off})$. This is then used to calculate the nES pulsation frequency during printing, $f = 1/(\tau_p)$. Finally, the total printed volume, v_{tot}, can be estimated as follows:

$$v_{tot} = (v_{est} \times f \times t_{pnt}) \qquad (2)$$

where t_{pnt} is the total spraying time, the time the nozzle voltage is held at V_2, which is user defined by the nES printing software.

2.5. Process characterisation and optimisation of the custom-made nES system

Clarification is needed for a few of the spraying parameters available from the nES system. The radius indicates the relative distance between the centre of a circle at the pre-set x and y coordinate to its perimeter, enabling polymer film deposition with dif-
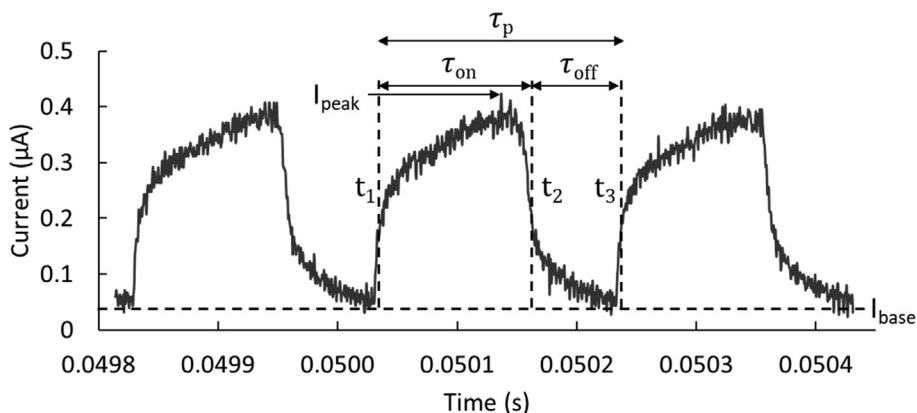
Fig. 4. Example current waveform of a 5% w/v zein solution captured during the nES that is used to calculate the spray volume per unit pulse.

ferent sizes as rings or dots. The number of rotations controls the number of layers of spray deposited on the surface, which primarily affects the film thickness. The dosing speed controls the speed of travel for the nozzle relative to the substrate, with a higher number implying a faster moving speed. The nozzle substrate distance (NSD) is the distance between the apex of the nozzle and the substrate, which is controlled by changing the distance travelled on the z-axis.

Three spraying parameters were investigated by the one-factor-at-time approach to understand their influence on deposited polymer film's width and thickness. These are NSD (ranging from 1.5 to 4.5 mm), dosing speeds (ranging from 10 to 40 mm/s) and the number of rotations (ranging from 10 to 40 turns). The characterisations of this section were performed using a conductive fluorine-doped tin oxide glass substrate as the deposition surfaces. Three rings of each experimental setting were prepared for surface profile measurement.

2.6. Surface profile measurement of zein films by a stylus profilometer

A Stylus Profilometer (DektakXT, Bruker, MA, USA) was used to measure the surface profile of dried nES zein films. The 'Hills and Valleys' profile was used for measurements and the 2 µm radius stylus was set at 1 mg stylus force. Three locations of the nES films were selected as shown in Fig. 5 to calculate the average spraying width and step height (thickness) of the polymer films, with a total number of nine measurements for each experimental setting.

Fig. 5. Locations on zine films where surface profile measurements were performed.

2.7. nES printing of zein solution on the soft hydrogel contact lenses

The commercial contact lenses (45% ocufilcon D/55% water) were removed from the packaging and soaked in PBS pH 7.4 for 30 min to equilibrate. A 3D-printed lens holder was made according to the specification of the contact lens. Excess liquid on the lens was removed by a lint-free dry wipe (RS Components, UK) before being transferred onto the 3D-printed lens holder. In example printing, the 5% zein (with 70% aqueous ethanol), referred as formulation Z3, solution was sprayed on the contact lens with the parameters as shown in Table 1.

2.8. Morphological studies of nES coated contact lenses

The surface morphology of nES zein coating on contact lenses was imaged using the Gemini 300 scanning electron microscopy (SEM) (Zeiss, Cambridge, UK) equipped with the PP3010T cryo-chamber (Quantum Design AG, Marly, Switzerland). The nES coated lenses were stored in a container with a lint-free wipe moistened with PBS before imagining. For the cryo-SEM experiments, the lens was cut to one-fourth of the whole lens, which was frozen rapidly by nitrogen slush. The frozen sample was transferred to the cryo-chamber for the sublimation of surface ice and sputter coating with platinum under vacuum before being sent to the SEM cold stage for image acquisition.

2.9. Optical transmittance of nES coated contact lenses

The transmission of light through contact lenses was adopted from the literature [38]. Briefly, the lenses were measured at a 1 nm interval from 200 to 800 nm using a UV–Vis spectrophotometer (Lambda 35, Perkin Elmer, UK). The light bean has a dimension of 7.5 mm in height and 1 mm in width according to the instrument specifications. Three contact lenses were coated as described above and immersed into a quartz cuvette containing PBS pH 7.4 solution to maintain hydration of contact lenses during measurement. The convex side of the contact lens was facing the incoming beam. Optical transparency of blank contact lenses was used as
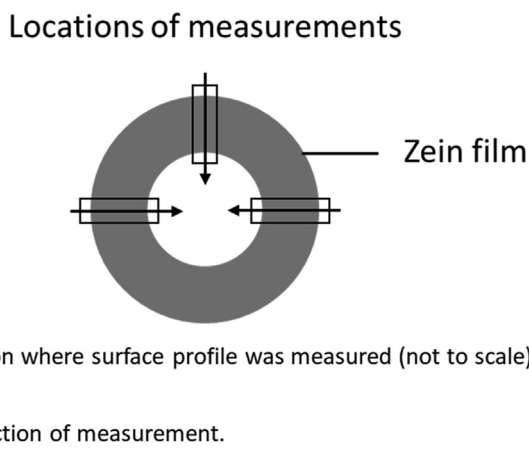
Table 1
nES spraying parameters of Z3 solution on the contact lens.

nES condition	1	2	3
Voltage (kV)	1.889	1.889	1.889
NSD (mm)	2.23	2.19	2.22
Spraying radius (mm)	4.5	5	5.5
Dosing speed (mm/s)	30	30	30
Number of revolutions	90	90	90

control. The lenses are expected to have at least 95% transmittance to provide a clear vision [39].

2.10. Determination of spray volume by UV–Vis spectrometry

As stated above, a stock solution of 5% w/v zein solution in 70% w/w aqueous ethanol (Z3) was prepared for this experiment. The stock solution was diluted to concentrations ranging from 0.2 mg/ml to 1 mg/ml to build a calibration curve, measured by the UV–Vis spectrophotometer Lambda 35 (PerkinElmer, Waltham, USA) at 278 nm. The stock solution was nanoelectrosprayed on an aluminium foil according to spraying parameters stated in Table 2. Three rings were prepared for each experimental setting. The coated foil was immediately immersed into 1 ml 70% w/w aqueous ethanol to quantify the amount of zein deposited on the foil, which was converted to volume by using the density equation, $\rho = m/v$, where ρ is the density, m is the mass and v is the volume. The results were compared with the volume calculated by the waveforms captured during the spraying event and the scaling law.

2.11. Statistical analysis

The basic calculation was performed by Microsoft Excel® (Microsoft Office 365). The data analysis was performed using SPSS statistical program (SPSS 25, IBM, New York, USA). Analysis of variance (ANOVA) and the Tukey test were used to compare the spraying width and thickness. A statistical significance is considered when the p-value is lower than 0.05.

3. Results and discussion

3.1. Effects of nES parameters on spraying width and film thickness

The physical properties of zein solutions used for nES are reported in Table 3. Two concentrations of zein solutions were prepared to understand the influence of polymer concentration on the film quality. The viscosity of Z1-2 (2.5% w/v) and Z3-4 (5% w/v) zein solutions decreased with increased ethanol concentration from 70% w/w to 80% w/w, showing a statistically significant difference ($p < 0.05$). The viscosity of a solution is dependent on the polymer concentration, the polymer's molecular weight and the solvent system.

The electrical conductivity was found to decrease with higher ethanol concentration in the solution for both concentrations of zein solutions. The electrical conductivity is also subjected to zein concentration, in which the 5 %w/v solutions have higher electrical conductivity than the corresponding 2.5 %w/v solutions. The electrical conductivity can influence the flow rate and ejected volume in nES operation [26], with the droplet size and volume inversely proportional to the conductivity. And hence, higher electrical conductivity tends to generate droplets with a smaller diameter. The surface tension for Z1-4 solutions is stated in Table 3 and shows no statistical difference between solutions. The surface tension primarily affects the strength of electric potential applied to the solution to break the liquid jet into fine droplets. The results above

showed a similar trend in literature that higher ethanol concentration in the zein solution leads to lower electrical conductivity, density, and viscosity [40].

Different nES process parameters were investigated to understand their influence on the spraying width and polymer film thickness after drying. Fig. 6 **A-B** shows the results of the influence of dosing speed for Z2 and Z4 solutions at 3.5 mm NSD with 10 rotations. The spraying width for Z2 and Z4 solution ranges from 4.46 to 4.86 mm and 4.74 to 4.96 mm, respectively. The thickness of films for Z2 and Z4 decreased with increasing dosing speed from 10 mm/s to 40 mm/s, showing an excellent fitting to the power-law ($R^2 > 0.99$) (Fig. 6**B**). With the increased dosing speed and the rest of the spraying parameters fixed, the overall spraying time and the total amount of material deposited on the substrate are reduced. The results indicate that the dosing speed primarily controls the thickness of the film and does not significantly affect the spraying width.

For multiple printing rotations, the spraying width and film thickness against the number of rotations for all solutions is shown in Fig. 6 **C-D**. The spraying width for both Z2 and Z4 did not show significant changes at different numbers of rotations. The spraying width ranges from 4.72 mm to 4.87 mm and 4.81 mm to 4.89 mm for Z2 and Z4, respectively. The film thickness increases from 0.21 μm (10 turns) to 0.9 μm (40 turns) and 0.32 μm (10 turns) to 1.26 μm (40 turns) for Z2 and Z4, correspondingly. The thickness of zein film for both concentrations show a linear relationship with the increased number of turns with a good correlation factor ($R^2 > 0.99$).

The effects of NSD on the spraying width and film thickness are shown in Fig. 6 **D-E**. The voltage was adjusted according to obtain a stable spray for different NSDs. For Z2, the spraying width increases from 1.81 mm at 1.5 mm NSD to 6.03 mm at 4.5 mm NSD. For Z4, the spraying width increases from 2.11 mm at 1.5 mm NSD to 6.58 mm at 4.5 mm NSD. It can be seen that the NSD is the main spraying parameter to determine the spraying width. Increasing NSD resulted in a broader spraying width with a positive linear relationship for both solutions and a good correlation factor ($R^2 > 0.99$). The thickness of films for Z2 and Z4 reduces accordingly with increased NSD and follows a linear relationship.

To optimise the spraying width and film thickness, the NSD is the first operational parameter that should be determined to achieve the desired spraying width according to the need. With the example of commercially available contact lenses used in the present work, the area for patterning was limited to a peripheral ring of around 3.1 mm width and 8 mm diameter to avoid coating the visual area of the lens. The NSD also controls the drying time of droplets generated by nES, which could affect the film morphology [41]. The higher NSD provides sufficient time for solvent evaporation, resulting in dry particles on the substrate. The NSD can influence the film morphology from ES deposition due to the solvent evaporation and drying process of in-flight droplets. For example, it has been reported that at a sufficiently large NSD the deposited particles are dry enough to stack on each other to form a rough film [21]. On the other hand, a smooth film can form when the NSD is low enough that the semi-dry nES droplets fuse on the substrate due to insufficient drying time [21]. Next, the dosing speed should be considered, which controls the thickness and might affect the drying time of the nES deposited droplets. Finally, the film thickness can be built up by changing the number of rotations to achieve the required thickness.

3.2. Effects of nES parameters on film surface profile

Two concentrations of zein were nanoelectrosprayed onto a conductive glass substrate to investigate the influence of polymer concentration on the morphology of the film. The general surface

Table 2
nES parameter of Z3 solution on aluminium foils.

nES condition	1	2	3
Voltage (kV)	2.2	2.2	2.2
NSD (mm)	2.5	2.5	2.5
Dosing speed (mm/s)	10	15	30
Number of revolutions	100	100	100
Spraying radius (mm)	5	5	5
Spraying time (s)	266	176	88

Table 3
Physical properties of zein solutions used for nES.

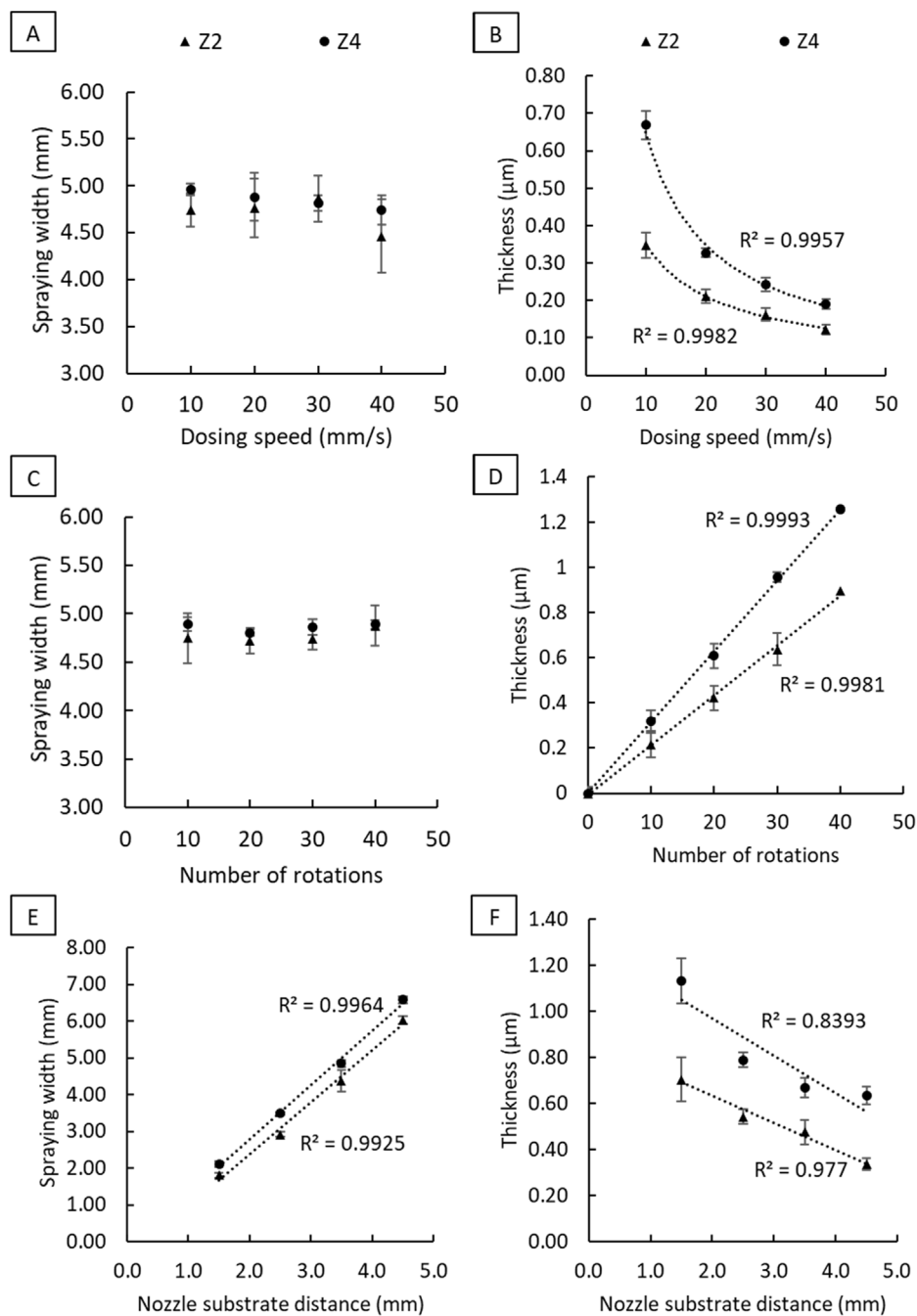|	Formulations			
	Z1	**Z2**	**Z3**	**Z4**
Zein (%w/v)	2.5	2.5	5	5
Ethanol (%w/w)	70	80	70	80
Conductivity (µS/cm)	200.0	186.2	333.0	293.0
Density ± SD (g/ml)	0.874 ± 0.001	0.848 ± 0.001	0.880 ± 0.001	0.857 ± 0.001
Surface tension ± SD (mN/m)	25.7 ± 1.0	24.9 ± 0.8	25.5 ± 1.2	24.7 ± 1.0
Viscosity ± SD (mPa.s)	4.20 ± 0.05	3.87 ± 0.06	5.60 ± 0.09	5.15 ± 0.05

Fig. 6. Spraying width and film thickness of Z2 (2.5% w/v) and Z4 (5% w/v) were affected by (A-B) nES dosing speed, (C-D) number of rotations and (E-F) nES NSD.

profiles of all zein solutions are shown in Fig. 7. Z1 and Z2 solutions (2.5% w/v zein) formed a thin film on a glass substrate with a twin peak pattern and a tough-like centre with relatively low thickness.

By doubling the concentration to 5% w/v (Z3-4), the material deposited formed a smoother surface profile with the absence of pronounced peaks.
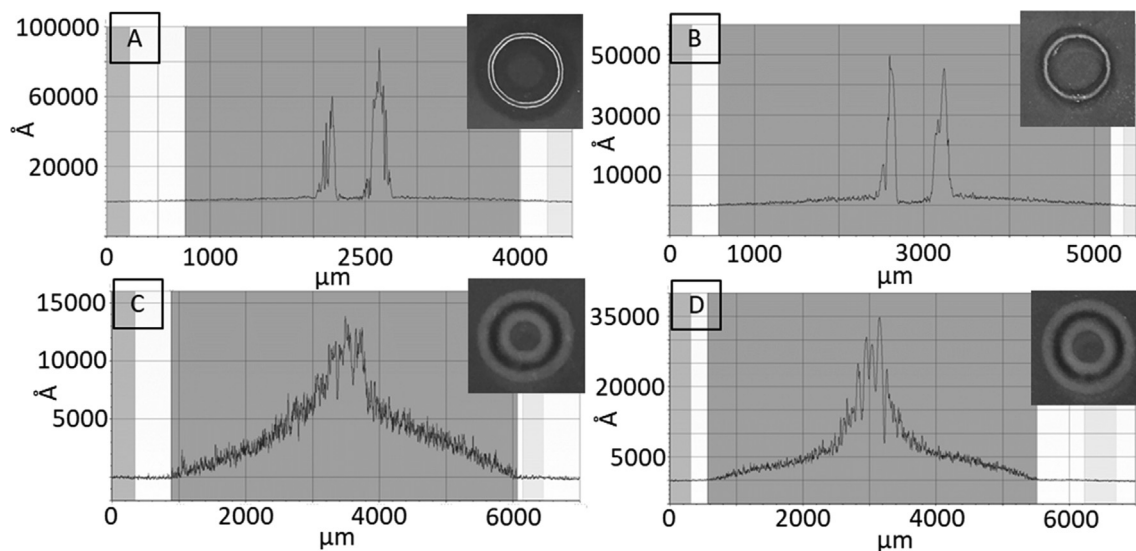
Fig. 7. The surface profile and the digital image of dried zein film deposited on the conductive glass substrate, (A) Z1, (B) Z2, (C) Z3 and (D) Z4.

The observed surface profiles can be explained by considering the spraying and drying processes. With the lower polymer concentration solutions (Z1 and Z2) a lower solution conductivity is observed which will lead to higher drop volumes and flow rate during deposition, resulting in fluid build-up and droplet coalescence to form the twin peak pattern and a tough-like centre at the central area of the film. The gradual decrease of the thickness of film from the centre to the edge could be accounted for by the accumulation of satellite droplets after solvent evaporation.

As for Z3-4, the smoother film thickness profile with increasing thickness towards the centre of the film can be explained by the lower droplet volume and spray flow rate resulting in the landing of semi-dried droplets without coalescence and bulk wetting. The higher central film thickness can be expected since the spraying solution formed a Taylor cone at the apex of the nozzle, followed by generating a fine plume of particles in a triangle shape, as shown in Fig. 1. The charged particles/droplets undergo Coulombic fission during the flight to the substrate, producing finer particles/-droplets landing further away from the centre of the film due to electrostatic repulsion [20]. The distance from the apex of the nozzle is the shortest distance from the centre of the film. Thus, the thickness of films is expected to be higher at the centre.

The effect of NSD on the observed uneven film thickness profile of Z2 solution was investigated. The surface profiles of Z2 with NSD from 1.5 mm to 4.5 mm are shown in Fig. 8. The twin peaks pattern remained in all surface profiles of the tested range of NSD, however, the distance between the peaks reduced gradually from 500 μm at 1.5 mm NSD (Fig. 8A) to 287 μm at 4.5 mm (Fig. 8D). The observation of a reduction in peak separation distance supports the explanation of a wetted central band followed by the coffee ring effect during drying as there will be more time for solvent evaporation in flight resulting in the formation of a narrower wetted band.

3.3. Zein solution deposition on commercial hydrogel contact lenses via nES

The target deposition area of zein by nES on a contact lens is shown in Fig. 9 **A**. A few factors were considered before coating on the soft contact lens. First, the coating area should not cover the vision zone of the contact lens to preserve the optical property of the lens. In general, the optical zone diameter of a contact lens is 8 mm to cover the pupil for all lighting conditions [42]. The vision zone of the contact lens was assumed to be 8 mm in this study,

leaving a 3.1 mm width at the peripheral region for coating. The NSD is known to be the main parameter affecting the spraying width and has a linear relationship with the spraying width (Fig. 6 **E**). The NSD was set to 2.2 mm from the contact lens surface which had been shown to produce a spray width of approximately 1.8 mm with the test solution. The radius parameter was then adjusted accordingly to avoid coating material deposited unnecessarily on the vision zone. The spraying radius is the distance from the centre of the lens to its perimeter from the top view. The optical transparency of contact lenses coated by zein (Fig. 9 **B**) with different spraying radii is shown in Fig. 9 **C**. The optical transparency is expected to be at least 95% or above at 600 nm to provide a clear vision. The results show that all coated contact lenses have optical transparency above 95% whereas the blank contact lens shows 98% transmittance. The optical transparency shows a trend that it reduces with a smaller spraying radius, which is likely due to the deposition of satellite drops close to the centre of the lens, partially blocking light passing through the contact lens. Different printed materials may affect transmittance to a greater extent and perform differently because of the change in conductivity of the spraying solution, which also affects the spray angle and the coverage of deposited material on the substrate. Therefore, the minimum radius needs to be determined. According to the results, it can be concluded that the minimum spraying radius should be kept above 4.5 mm at 2.2 mm NSD.

The results of nES 5% w/v zein solution (Z3) on contact lenses with a range of radii are shown in Fig. 10. Fig. 10**A, C and E**. The white ring indicates the zein coating on contact lenses and the centre of the lens remained free of zein polymer at different spraying radii. The SEM images (Fig. 10**B, D and F**) confirm that no zein polymer was deposited at the centre of the lens and was confined observed in the peripheral region. Fig. 10 **G** shows the cross-sectional image of an example contact lens after coating zein polymer in the peripheral region. A dense film of zein film adhered to the peripheral region of the lens. Overall, the results show that the nES process can deposit the model polymer selectively at the target area and avoid coating the visual axis.

3.4. nES deposited volume measurement: Comparison of experimental data and theoretical prediction

The quantity of zein deposited on aluminium foil substrates was compared with the theoretically predicted quantity, yielded from
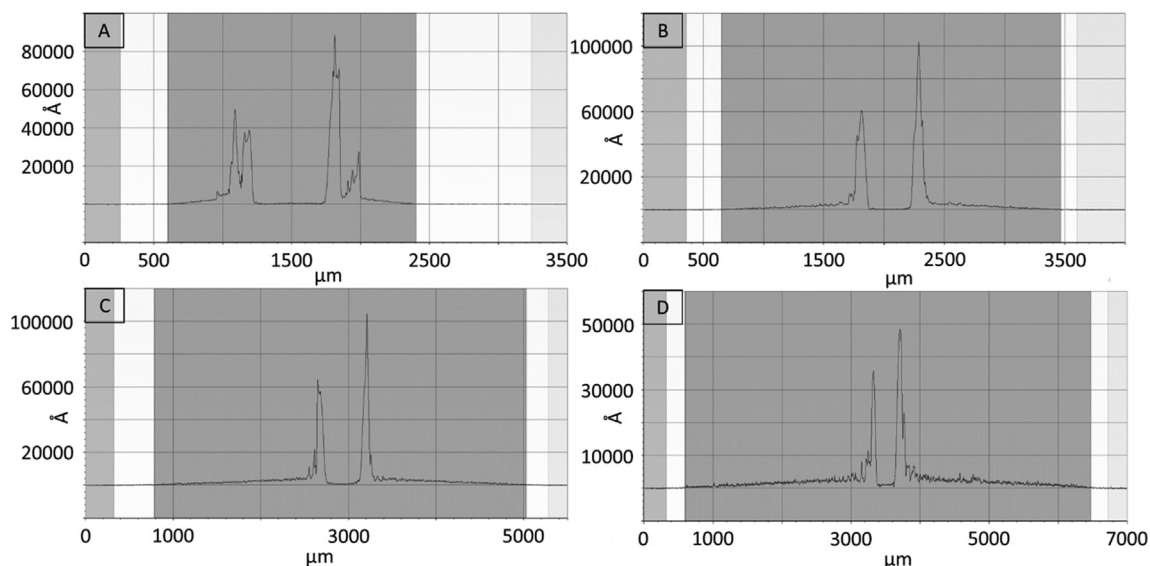
Fig. 8. The surface profile of dried zein films prepared by the Z2 solution at different NSD, (A) 1.5 mm, (B) 2.5 mm, (C) 3.5 mm and (D) 4.5 mm.
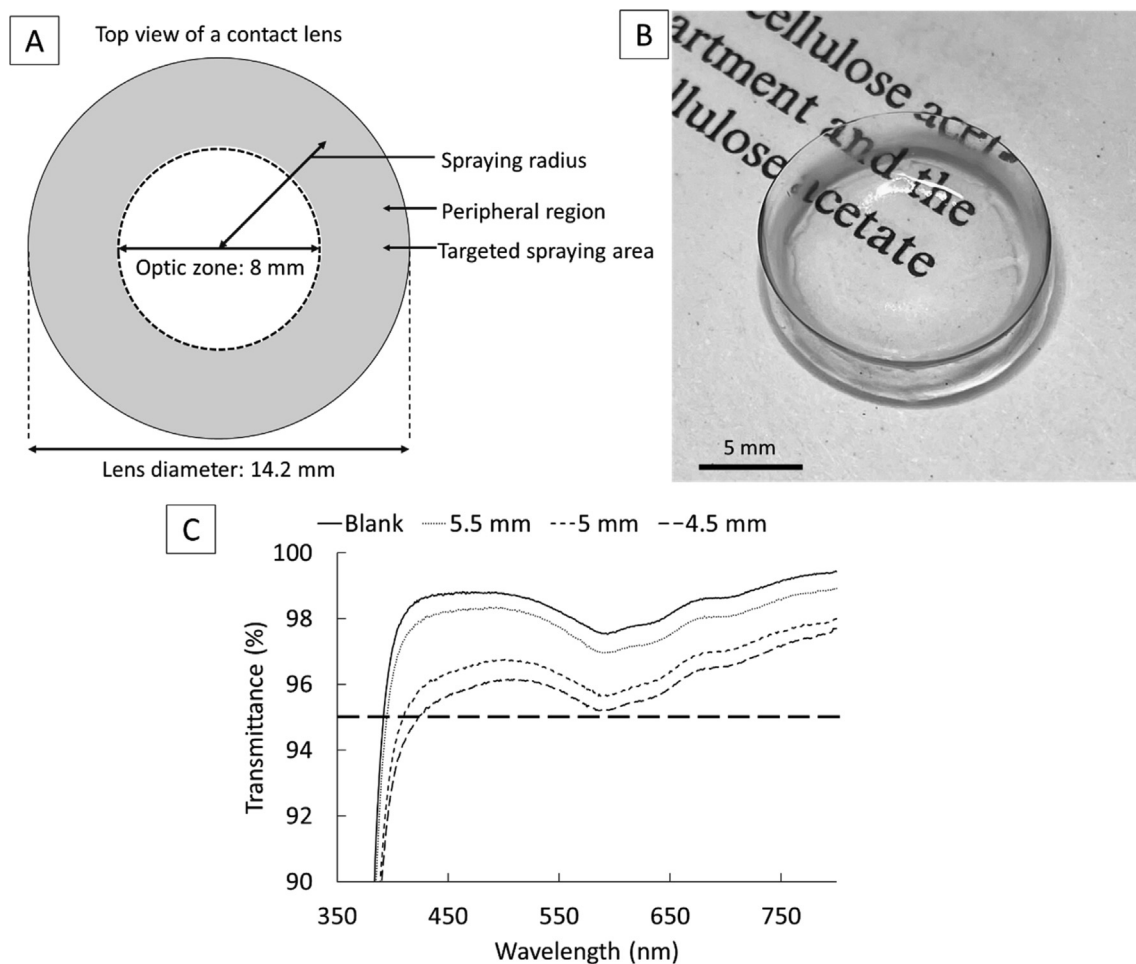

Fig 9. (A) Illustration of the targeted spraying area on the contact lens; (B) a digital image of a zein coated contact lens on a piece of newspaper. The white ring at the peripheral region of the contact lens is the zein polymer deposited by nES; (C) optical transparency of blank contact lenses and zein coated contact lenses with different spraying radii.

the processing of current transients captured during the spraying process as described in method section 2.4. A UV–Vis spectrometer was used to independently quantify the amount of zein deposited on the substrate. Results from Z3 solution are presented as deposited solution volume against total spray time in Fig. 11. As shown, both the experimentally measured and theoretically estimated
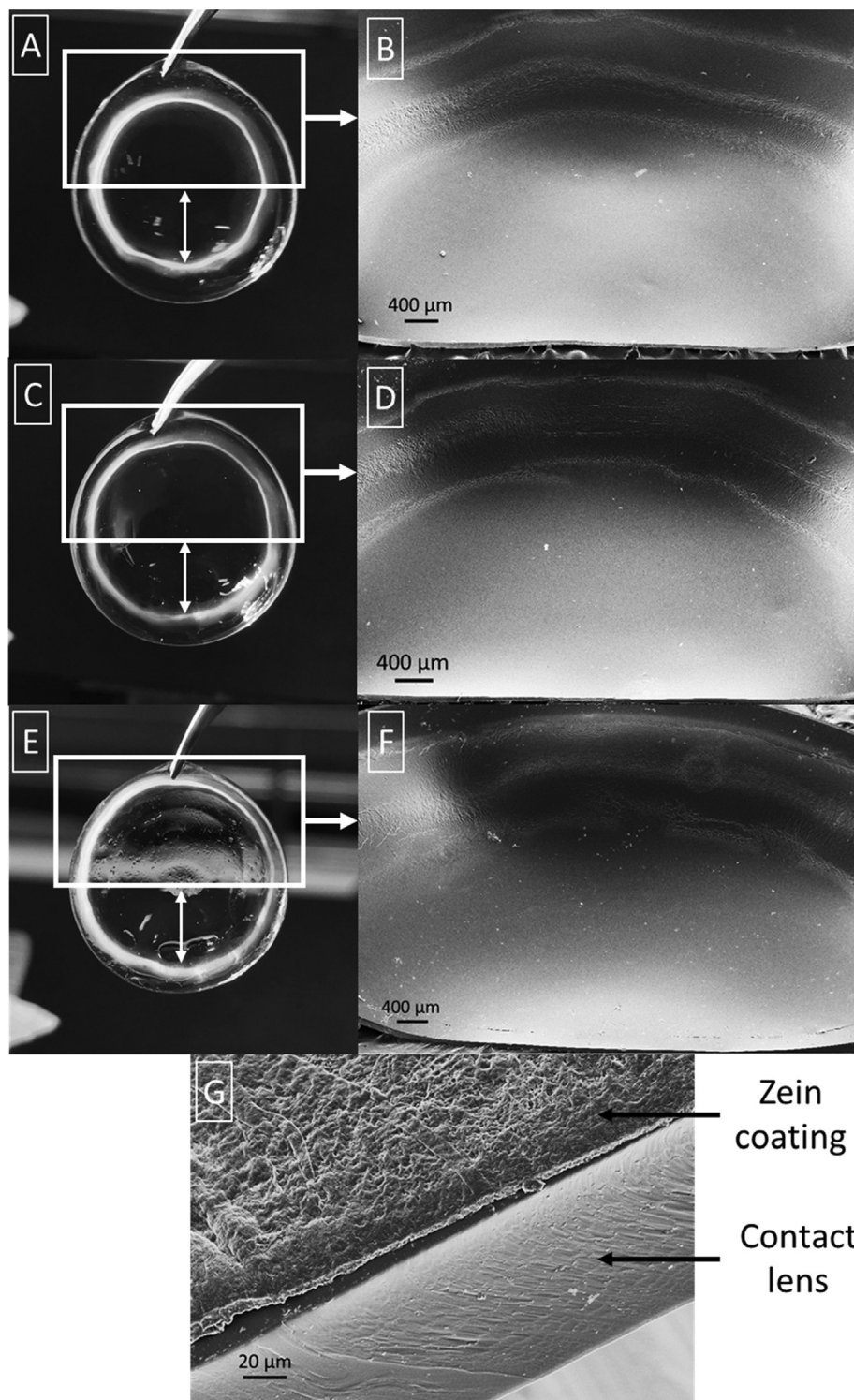
Fig. 10. Digital images of 5% w/v zein (Z3) coated lenses with different spraying radii (indicated by the white arrows); A: 4.5 mm spraying radius, C: 5 mm spraying radius and E: 5.5 mm spraying radius. B, D and E are the SEM images of the surfaces of zein coated contact lenses. G: Example cross-sectional SEM image of the zein coated contact lens.

printed zein volumes are linearly proportional to the total spray time with a good correlation factor ($R^2 > 0.99$), however, the amount of zein quantified by the UV–Vis method is found to be consistently lower than the amount from the transient estimation method.

The scaling law by De La Mora [29,30], which is then adapted by Paine et al. [22] in Eq. (1), provides a good scaling of spray current with volumetric flow rate in ES but for a particular spray fluid only gives an order of magnitude estimation of the absolute spray current values at a particular flow rate. Therefore, in order to improve accuracy of material/drug dosing in the printed coating in the present work it was necessary to include an empirical derived constant, A, to enable accurate correlation of ejected charge measurements to deposit volume. For this reason, equation (2) is
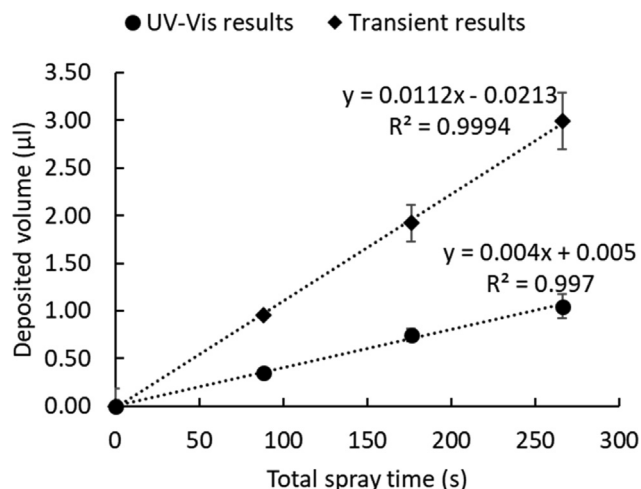
Fig. 11. Amount of zein solution quantified by the UV–Vis spectroscopy compared with the estimated volume by scaling law.

modified to include constant A, an experimentally derived constant from best fit trendlines, to give an accurate volume estimate from the transient technique:

$$v_{tot} = A.v_{est}.f.t_{pnt} \qquad (3)$$

For the zein solutions tested in this study, the experimentally determined value of A, to give a correlation between the transient technique and UV–Vis measurements, was found to be 0.36. The theoretical data with and without experiment constant are shown in Table 4. The spray volume of zein solution measured by UV–Vis was found to range from 1.049 to 0.346 μl over the range of spraying time. Applying the experimental constant to the transient data, the spray volume is estimated to range from 1.079 to 0.344 μl. In these cases, equation (3) can be useful to predict the spray volume by using the current waveform captured during the spraying process.

It is worth mentioning that there is no upper limit on the maximum coating thickness that can be deposited. The technique enables multiple print layers, and the thickness can be adjusted by changing the polymer concentration, dosing speed, NSD and the number of print rotations. The maximum deposition volume in a single experiment is controlled by the volume of the precursor liquid reservoir used, which is 2.5 ml in the experimental setup of this study. The deposition volume of a single layer of the polymer coating investigated in this study was within nanolitre range. When depositing drug-containing formulas, as the processability is controlled by the conductivity and viscosity of the spraying solution, the polymer can be replaced completely by the drug, as long as the spraying solution retains suitable physical properties for nES.

Table 4
Theoretical and experimental calculations of the deposited volume of zein solutions with different total spraying time.

	Total spraying time (s)		
	266	176	88
UV–Vis results (μl)	1.049 ± 0.061	0.746 ± 0.124	0.346 ± 0.066
Transient results before correction (μl)	2.997 ± 0.181	1.920 ± 0.298	0.954 ± 0.195
Transient results after correction (μl)	1.079 ± 0.065	0.691 ± 0.107	0.344 ± 0.070

4. Conclusion

This study demonstrated for the first time the highly controllable deposition of polymeric liquid formulations on soft and curved hydrogel-based substrates using nES in pre-defined shape patterns at pre-determined locations. Using commercial soft contact lenses as a challenging example with wet and curved surfaces, the controlled deposition of model polymer zein solution in a ring shape at the peripheral region of the contact lens without blocking the vision zone was demonstrated. The NSD is the most significant factor controlling the coating coverage and should be considered first for the process optimisation, followed by adjusting the polymer concentration, dosing time, and the number of revolutions to increase the coating thickness. The deposition volume was shown to be highly predictable by using spray current transients with the established electrospray scaling laws, which is critical for precise drug dosing for medical applications. The on-demand nature of nES minimises the waste of materials compared to other methods to prepare DECLs while maintaining a clear optical zone. The present study shows the potential of nES as a platform technology for material deposition on medical devices with challenging features such as wet, soft and curved surfaces. It is envisaged that the applications are primarily for functional coating of medical devices, with examples of drug delivery and anti-microbial surface treatment. For drug delivery applications, the drug candidates for coating range from small molecules to macromolecules including peptides and proteins as long as a suitable solvent can be used to ensure the stability of the drug molecules.

Declaration of Competing Interest

The authors declare that they have no known competing financial interests or personal relationships that could have appeared to influence the work reported in this paper.

Acknowledgement

References

[1] I.P. Kaur, S. Kakkar, Nanotherapy for posterior eye diseases, J. Control. Release. 193 (2014) 100–112, https://doi.org/10.1016/j.jconrel.2014.05.031.

[2] V. Agrahari, A. Mandal, V. Agrahari, H.M. Trinh, M. Joseph, A. Ray, H. Hadji, R. Mitra, D. Pal, A.K. Mitra, A comprehensive insight on ocular pharmacokinetics, Drug Deliv. Transl. Res. 6 (2016) 735–754, https://doi.org/10.1007/s13346-016-0339-2.

[3] R. Kholdebarin, R.J. Campbell, Y.P. Jin, Y.M. Buys, G. Beiko, C. Birt, K. Damji, F. Feldman, C. Lajoie, S. Kulkarni, J. Martow, T. Sakamoto, J. Spencer, G.E. Trope, Multicenter study of compliance and drop administration in glaucoma, Can. J. Ophthalmol. 43 (2008) 454–461, https://doi.org/10.3129/I08-076.

[4] P.A. Newman-Casey, A.L. Robin, T. Blachley, K. Farris, M. Heisler, K. Resnicow, P. P. Lee, The Most Common Barriers to Glaucoma Medication Adherence: A Cross-Sectional Survey, Ophthalmology 122 (2015) 1308–1316, https://doi.org/10.1016/j.ophtha.2015.03.026.

[5] P.A. Newman-Casey, L.M. Niziol, B.W. Gillespie, N.K. Janz, P.R. Lichter, D.C. Musch, The Association between Medication Adherence and Visual Field Progression in the Collaborative Initial Glaucoma Treatment Study, Ophthalmology 127 (2020) 477–483, https://doi.org/10.1016/j.ophtha.2019.10.022.

[6] J. Thygesen, Glaucoma therapy: Preservative-free for all?, Clin Ophthalmol. 12 (2018) 707–717, https://doi.org/10.2147/OPTH.S150816.

[7] S.A. Davis, B. Sleath, D.M. Carpenter, S.J. Blalock, K.W. Muir, D.L. Budenz, Drop instillation and glaucoma, Curr. Opin. Ophthalmol. 29 (2018) 171–177, https://doi.org/10.1097/ICU.0000000000000451.

[8] R. Gupta, B. Patil, B.M. Shah, S.J. Bali, S.K. Mishra, T. Dada, Evaluating Eye Drop Instillation Technique in Glaucoma Patients, J. Glaucoma. 21 (2012) 189–192, https://doi.org/10.1097/IJG.0b013e31820bd2e1.

[9] K.H. Hsu, S. Gause, A. Chauhan, Review of ophthalmic drug delivery by contact lenses, J. Drug Deliv. Sci. Technol. 24 (2014) 123–135, https://doi.org/10.1016/S1773-2247(14)50021-4.

[10] J. Xu, Y. Xue, G. Hu, T. Lin, J. Gou, T. Yin, H. He, Y. Zhang, X. Tang, A comprehensive review on contact lens for ophthalmic drug delivery, J. Control. Release. 281 (2018) 97–118, https://doi.org/10.1016/j.jconrel.2018.05.020.

[11] J. Vision, Johnson & Johnson Vision Care Receives FDA Approval for ACUVUE® Theravision™ with Ketotifen – World's First and Only Drug-Eluting Contact Lens, (2022). https://www.jjvision.com/press-release/johnson-johnson-vision-care-receives-fda-approval-acuvuer-theravisiontm-ketotifen (accessed April 24, 2022).

[12] A. Soluri, A. Hui, L. Jones, Delivery of ketotifen fumarate by commercial contact lens materials, Optom. Vis. Sci. 89 (2012) 1140–1149, https://doi.org/10.1097/OPX.0b013e3182639dc8.

[13] C.C. Li, A. Chauhan, Ocular transport model for ophthalmic delivery of timolol through p-HEMA contact lenses, J. Drug Deliv. Sci. Technol. 17 (2007) 69–79, https://doi.org/10.1016/S1773-2247(07)50010-9.

[14] F. Yan, Y. Liu, S. Han, Q. Zhao, N. Liu, Bimatoprost Imprinted Silicone Contact Lens to Treat Glaucoma, AAPS PharmSciTech. 21 (2020), https://doi.org/10.1208/s12249-020-1622-6.

[15] A.R. Desai, F.A. Maulvi, D.M. Desai, M.R. Shukla, K.M. Ranch, B.A. Vyas, S.A. Shah, S. Sandeman, D.O. Shah, Multiple drug delivery from the drug-implants-laden silicone contact lens: Addressing the issue of burst drug release, Mater. Sci. Eng. C. 112 (2020) 110885, https://doi.org/10.1016/j.msec.2020.110885.

[16] J.H. Choi, Y. Li, R. Jin, T. Shrestha, J.S. Choi, W.J. Lee, M.J. Moon, H.T. Ju, W. Choi, K.C. Yoon, The Efficiency of Cyclosporine A-Eluting Contact Lenses for the Treatment of Dry Eye, Curr. Eye Res. 44 (2019) 486–496, https://doi.org/10.1080/02713683.2018.1563702.

[17] O.L. Lanier, K.G. Christopher, R.M. Macoon, Y. Yu, P. Sekar, A. Chauhan, Commercialization challenges for drug eluting contact lenses, Expert Opin. Drug Deliv. 00 (2020) 1–17, https://doi.org/10.1080/17425247.2020.1787983.

[18] P. Mehta, A.A. Al-Kinani, M.S. Arshad, M.W. Chang, R.G. Alany, Z. Ahmad, Development and characterisation of electrospun timolol maleate-loaded polymeric contact lens coatings containing various permeation enhancers, Int. J. Pharm. 532 (2017) 408–420, https://doi.org/10.1016/j.ijpharm.2017.09.029.

[19] Y. Liu, S. Li, H. Li, M.d. Alomgir Hossen, D.E. Sameen, J. Dai, W. Qin, KangJu Lee, Synthesis and properties of core-shell thymol-loaded zein/shellac nanoparticles by coaxial electrospray as edible coatings, Mater. Des. 212 (2021) 110214, https://doi.org/10.1016/j.matdes.2021.110214.

[20] E. Bodnár, J. Grifoll, J. Rosell-Llompart, Polymer solution electrospraying: A tool for engineering particles and films with controlled morphology, J. Aerosol Sci. 125 (2018) 93–118, https://doi.org/10.1016/j.jaerosci.2018.04.012.

[21] A. Jaworek, Electrospray droplet sources for thin film deposition, J. Mater. Sci. 42 (2007) 266–297, https://doi.org/10.1007/s10853-006-0842-9.

[22] D.N. Nguyen, C. Clasen, G. Van den Mooter, Pharmaceutical Applications of Electrospraying, J. Pharm. Sci. 105 (2016) 2601–2620, https://doi.org/10.1016/j.xphs.2016.04.024.

[23] M. Wilm, M. Mann, Analytical properties of the nanoelectrospray ion source, Anal. Chem. 68 (1996) 1–8, https://doi.org/10.1021/ac9509519.

[24] G.T.T. Gibson, S.M. Mugo, R.D. Oleschuk, Nanoelectrospray emitters: Trends and perspective, Mass Spectrom. Rev. 28 (2009) 918–936, https://doi.org/10.1002/mas.20248.

[25] M.S. Alexander, M.D. Paine, J.P.W. Stark, Pulsation modes and the effect of applied voltage on current and flow rate in nanoelectrospray, Anal. Chem. 78 (2006) 2658–2664, https://doi.org/10.1021/ac0520036.

[26] M.D. Paine, M.S. Alexander, K.L. Smith, M. Wang, J.P.W. Stark, Controlled electrospray pulsation for deposition of femtoliter fluid droplets onto surfaces, J. Aerosol Sci. 38 (2006) 315–324, https://doi.org/10.1016/j.jaerosci.2006.12.004.

[27] C. Wei, H. Qin, C.P. Chiu, Y.S. Lee, J. Dong, Drop-on-demand E-jet printing of continuous interconnects with AC-pulse modulation on highly insulating substrates, J. Manuf. Syst. 37 (2015) 505–510, https://doi.org/10.1016/j.jmsy.2014.07.005.

[28] H. Qin, Y. Cai, J. Dong, Y.S. Lee, Direct printing of capacitive touch sensors on flexible substrates by additive e-jet printing with silver nanoinks, J. Manuf. Sci. Eng. Trans. ASME 139 (2017) 1–7, https://doi.org/10.1115/1.4034663.

[29] H. Chen, J. Zhong, J. Wang, R. Huang, X. Qiao, H. Wang, Z. Tan, Enhanced growth and differentiation of myoblast cells grown on E-jet 3D printed platforms, Int. J. Nanomed. 14 (2019) 937–950, https://doi.org/10.2147/IJN.S193624.

[30] M.J. Poellmann, K.L. Barton, S. Mishra, A.J.W. Johnson, Patterned Hydrogel Substrates for Cell Culture with Electrohydrodynamic Jet Printing, Macromol. Biosci. 11 (2011) 1164–1168, https://doi.org/10.1002/mabi.201100004.

[31] K. Kim, G. Kim, B.R. Lee, S. Ji, S.Y. Kim, B.W. An, M.H. Song, J.U. Park, High-resolution electrohydrodynamic jet printing of small-molecule organic light-emitting diodes, Nanoscale 7 (2015) 13410–13415, https://doi.org/10.1039/c5nr03034j.

[32] D.A. Kovacevich, L. Lei, D. Han, C. Kuznetsova, S.E. Kooi, H. Lee, J.P. Singer, Self-Limiting Electrospray Deposition for the Surface Modification of Additively Manufactured Parts, ACS Appl. Mater. Interfaces 12 (2020) 20901–20911, https://doi.org/10.1021/acsami.9b23544.

[33] J. Fernández De La Mora, On the outcome of the Coulombic fission of a charged isolated drop, J. Colloid Interface Sci. 178 (1996) 209–218, https://doi.org/10.1006/jcis.1996.0109.

[34] J.F. de la Mora, I.G. Loscertales, The current emitted by highly conducting Taylor cones, J. Fluid Mech. 260 (1994) 155–184, https://doi.org/10.1017/S0022112094003472.

[35] P.M. Silva, S. Torres-Giner, A.A. Vicente, M.A. Cerqueira, Electrohydrodynamic processing for the production of zein-based microstructures and nanostructures, Curr. Opin. Colloid Interface Sci. 56 (2021), https://doi.org/10.1016/j.cocis.2021.101504 101504.

[36] M. Wang, D. Li, J. Li, S. Li, Z. Chen, D.G. Yu, Z. Liu, J.Z. Guo, Electrospun Janus zein–PVP nanofibers provide a two-stage controlled release of poorly water-soluble drugs, Mater. Des. 196 (2020) 109075, https://doi.org/10.1016/j.matdes.2020.109075.

[37] E. Corradini, P.S. Curti, A.B. Meniqueti, A.F. Martins, A.F. Rubira, E.C. Muniz, Recent advances in food-packing, pharmaceutical and biomedical applications of zein and zein-based materials, Int. J. Mol. Sci. 15 (2014) 22438–22470, https://doi.org/10.3390/ijms151222438.

[38] N.M. Quesnel, P. Simonet, Spectral transmittance of UV-absorbing soft and rigid gas permeable contact lenses, Optom. Vis. Sci. 72 (1995) 2–10, https://doi.org/10.1097/00006324-199501000-00002.

[39] F.A. Maulvi, R.J. Patil, A.R. Desai, M.R. Shukla, R.J. Vaidya, K.M. Ranch, B.A. Vyas, S.A. Shah, D.O. Shah, Effect of gold nanoparticles on timolol uptake and its release kinetics from contact lenses: In vitro and in vivo evaluation, Acta Biomater. 86 (2019) 350–362, https://doi.org/10.1016/j.actbio.2019.01.004.

[40] F. Rodríguez-Félix, C.L. Del-Toro-Sánchez, F. Javier Cinco-Moroyoqui, J. Juárez, S. Ruiz-Cruz, G.A. López-Ahumada, E. Carvajal-Millan, D.D. Castro-Enríquez, C.G. Barreras-Urbina, J.A. Tapia-Hernández, Preparation and Characterization of Quercetin-Loaded Zein Nanoparticles by Electrospraying and Study of In Vitro Bioavailability, J. Food Sci. 84 (2019) 2883–2897, https://doi.org/10.1111/1750-3841.14803.

[41] N. Bock, T.R. Dargaville, M.A. Woodruff, Electrospraying of polymers with therapeutic molecules: State of the art, Prog. Polym. Sci. 37 (2012) 1510–1551, https://doi.org/10.1016/j.progpolymsci.2012.03.002.

[42] A. Abass, S. Stuart, B.T. Lopes, D. Zhou, B. Geraghty, R. Wu, S. Jones, I. Flux, R. Stortelder, A. Snepvangers, R. Leca, A. Elsheikh, C. Boote, Simulated optical performance of soft contact lenses on the eye, PLoS ONE 14 (5) (2019) 1–17, https://doi.org/10.1371/journal.pone.0216484.